J. Soc. Cosmet. Sci. Korea
Vol. 47, No. 2, June 2021, 107-121

pISSN 1226-2587
eISSN 2288-9507
http://dx.doi.org/10.15230/SCSK.2021.47.2.107

B16/F10 흑색종 세포에서 S-Adenosylhomocysteine Hydrolase의 선택적 저해제 3-Deazaneplanocin A에 의한 멜라닌 생성 증진

황 윤 정* · 부 용 출**,†

*경북대학교 의학전문대학원 분자의학교실, 대학원생
**경북대학교 의학전문대학원 분자의학교실, 교수
(2021년 3월 10일 접수, 2021년 4월 12일 수정, 2021년 5월 14일 채택)

Melanogenesis Promotion by 3-Deazaneplanocin A, a Specific Inhibitor of S-Adenosylhomocysteine Hydrolase, in B16/F10 Melanoma Cells

Yun Jeong Hwang and Yong Chool Boo†

Department of Molecular Medicine, School of Medicine, Brain Korea (BK) 21 Plus Kyungpook National University (KNU) Biomedical Convergence Program, Cell and Matrix Research Institute, Kyungpook National University, Daegu 41944, Korea
(Received March 10, 2021; Revised April 12, 2021; Accepted May 14, 2021)

요 약: 백색증이나 백반증에서 관찰되는 피부 저색소침착은 유전적 요인, 후성유전적 요인 및 기타 요인에 의해 멜라닌 합성이 감소할 때 발생한다. 세포에서 멜라닌 합성을 촉진 할 수 있는 약물 후보를 확인하기 위해 141개의 세포 투과성 저분자 약물로 구성된 후성유전적 조절제 라이브러리를 스크리닝했다. B16/F10 쥐 흑색종 세포를 0.1 ㎛M에서 각 약물로 처리하고 멜라닌 합성 및 세포 생존력을 모니터링했다. 그 결과, (−)-네플라노신 A, 3-디아자네플라노신 A (DZNep) 및 DZNep 염산염이 세포 독성을 일으키지 않고 멜라닌 합성을 증가시키는 것으로 나타났다. 이 세 가지 구조적으로 관련된 약물은 세포 멜라닌 합성 및 세포 생존력에 유사한 용량 의존적 효과를 나타내었기 때문에 DZNep을 추가 실험을 위한 대표 약물로 선택하였다. DZNep는 세포내 멜라닌 함량과 티로시나제(TYR) 활성을 증가 시켰다. DZNep은 또한 mRNA와 단백질 수준에서 TYR, 티로시나제 관련 단백질 1 (TYRP1) 및 도파크롬 토토머라제 (DCT)의 발현을 유도했다. DZNep는 또한 멜라닌 합성의 주요 조절자인 소안구증 관련 전사 인자(MITF)의 mRNA와 단백질 발현을 유도했다. DZNep은 S-아데노실 호모시스테인 가수분해효소의 선택적 억제제이며 히스톤 메틸화효소를 저해하는 S-아데노실 호모시스테인의 세포내 축적을 유발하였다. 이 연구는 특정 세포 상황에서 S-아데노실 호모시스테인 가수분해효소를 표적함으로써 멜라닌 생성이 조절될 수 있음을 시사한다.

Abstract: Skin hypopigmentation, which is observed in albinism or vitiligo, occurs when melanin synthesis is decreased by genetic, epigenetic, and other factors. To identify drug candidates that can promote melanin synthesis in cells, we screened an epigenetic modulator library consisting of 141 cell-permeable, small molecule drugs. B16/F10 murine melanoma cells were treated with each drug at 0.1 μM and melanin synthesis and cell viability were subsequently monitored. As a result, (−)-neplanocin A, 3-deazaneplanocin A (DZNep), and DZNep hydrochloride were found to increase cellular melanin synthesis without causing cytotoxicity. Because these three structurally related drugs exhibited similar dose-dependent effects

† 주 저자 (e-mail: ycboo@knu.ac.kr)
call: 053-420-4946

on melanin synthesis and cell viability, DZNep was selected as a representative drug for additional experiments. DZNep increased intracellular melanin content and tyrosinase (TYR) activity. DZNep also induced the expression of TYR, tyrosinase-related protein 1 (TYRP1), and dopachrome tautomerase (DCT) at the mRNA and protein levels. DZNep also induced the mRNA and protein expression of microphthalmia-associated transcription factor (MITF), a key regulator of melanin synthesis. DZNep is a specific inhibitor of S-adenosylhomocysteine hydrolase and it caused the accumulation of S-adenosylhomocysteine that inhibits histone methyltransferases in cells. This study suggests that melanogenesis can be modulated by targeting S-adenosylhomocysteine hydrolase in certain cellular contexts.

Keywords: *promelanogenic, 3-deazaneplanocin A, epigenetic, histone methyltransferase, S-adenosylhomocysteine hydrolase*

1. Introduction

Pigmentary disorders resulting from over-, or under-production of melanin represent a significant research area in dermatology, not only for aesthetics but also from a clinical viewpoint[1,2]. Hyperpigmentation occurs when melanin synthesis is abnormally increased in certain circumstances[3]. Melanin synthesis and accumulation may be caused by inflammation and intrinsic or photo-aging of the skin[4]. Hypopigmentation occurs when melanin synthesis is reduced by genetic or epigenetic variations, as in the cases of albinism and vitiligo[5,6]. Although skin pigmentary disorders are not considered life-threatening, they can cause severe mental stress and significantly diminish the quality of life[7].

Melanin synthesis begins with the tyrosinase (TYR)-catalyzed oxidation of L-tyrosine or L-dihydroxyphenylalanine (DOPA), followed by the production of pheomelanin or eumelanin depending on the intermediate process[8-10]. Microphthalmia-associated transcription factor (MITF) plays a primary role in inducing gene expression of melanogenic enzymes such as TYR, tyrosinase-related protein 1 (TYRP1), and dopachrome tautomerase (DCT) in response to various stimuli[11]. Various approaches have been tried to modulate melanin synthesis and pigmentation using peptides, amino acids, and their analogs[12]. In addition, various natural and synthetic products have been shown to suppress or promote melanin synthesis and pigmentation[13-17].

Inherited skin color is largely determined by genetic traits such as polymorphisms in the solute carrier family 24 member 5 (SLC24A5) and solute carrier family 24 member 5 (SLC24A5) genes[18,19]. Epigenetic mechanisms, such as DNA methylation, histone modification, and microRNA expression also contribute to long-term changes in skin color[20]. Recent studies have shown that melanin synthesis may be regulated by various epigenetic modulators. For example, 5-azacytidine, a DNA methylation inhibitor, reduced melanin levels in Mel-Ab cells by downregulating MITF and its regulatory target, TYR[21]. Histone deacetylase inhibitors including trichostatin A repress cellular melanin synthesis through transcriptional downregulation of the melanocyte-specific isoform of MITF (M-MITF) in melanocytes and melanoma, and topical treatment of trichostatin A decreased skin pigmentation in mice[22]. Among the microRNAs, miR-125b, which targets SRC homology 3 domain-binding protein 4 (SH3BP4), decreased melanin levels[23,24].

Previously, we screened an epigenetic modulator library to identify new drug candidates that can suppress cellular melanin synthesis[25]. In the present study, we used the same drug library for screening assays, but for a different purpose to identify drug candidates that can promote cellular melanin synthesis. As a result, 3-deazaneplanocin A (DZNep) and other structurally related drugs were found to promote cellular melanin synthesis. DZNep was shown to induce the expression of melanogenic enzymes, such as TYR, through a mechanism mediated by MITF. DZNep is a specific inhibitor of S-adenosylhomocysteine hydrolase and it caused the accumulation of S-adenosylhomocysteine in the treated cells[26,27]. This study suggests that melanogenesis can be modulated by targeting S-adenosylhomocysteine hydrolase in certain cellular contexts.

2. Materials and Methods

2.1. An Epigenetic Screening Library

An epigenetic screening library (Item No. 11076), purchased

from Cayman Chemical (USA), was used in the preliminary screening assays. The library contained 141 cell-permeable, small molecules that potentially cause epigenetic changes in cells. Its composition is shown in Table 1.

Table 1. Epigenetic screening library used in this study

Code	CAS number	Drug name	Code	CAS number	Drug name
1	21293-29-8	(+)-Abscisic acid	38	1020149-73-8	SGI-1027
2	3544-24-9	3-Amino benzamide	39	2353-33-5	Decitabine
3	929016-96-6	SB939	40	1300031-49-5	I-BET151
4	950762-95-5	PCI 34051	41	1268524-70-4	(+)-JQ1
5	1219807-87-0	4-Iodo-SAHA	42	1268524-71-5	(−)-JQ1
6	410536-97-9	Sirtinol	43	160003-66-7	BSI-201
7	328968-36-1	C646	44	86-55-5	1-Naphthoic acid
8	1239262-52-2	Tubastatin A (trifluoroacetate salt)	45	1716-12-7	Sodium 4-phenylbutyrate
9	78824-30-3	Garcinol	46	459868-92-9	Rucaparib (phosphate)
10	476-66-4	Ellagic acid	47	5852-78-8	IOX1
11	287383-59-9	Scriptaid	48	1271738-62-5	MI-2 (hydrochloride)
12	183506-66-3	Apicidin	49	1934302-23-4	MI-nc (hydrochloride)
13	83209-65-8	HC toxin	50	95058-81-4	Gemcitabine
14	1238673-32-9	UNC0321 (trifluoroacetate salt)	51	192441-08-0	Lomeguatrib
15	72877-50-0	(−)-Neplanocin A	52	1216744-19-2	GSK4112
16	1373232-26-8	Cl-amidine (hydrochloride)	53	876150-14-0	Octyl-α-ketoglutarate
17	877617-46-4	F-amidine (trifluoroacetate salt)	54	1596-84-5	Daminozide
18	1256375-38-8	JGB1741	55	1797832-71-3	GSK-J1 (sodium salt)
19	1260635-77-5	coumarin-SAHA	56	2108665-15-0	GSK-J2 (sodium salt)
20	1260907-17-2	I-BET762	57	1797983-09-5	GSK-J4 (hydrochloride)
21	1255580-76-7	UNC0638	58	112522-64-2	CI-994
22	880487-62-7	Phthalazinone pyrazole	59	2108899-91-6	CPTH2 (hydrochloride)
23	961-29-5	Isoliquiritigenin	60	33419-42-0	Etoposide
24	1207113-88-9	CCG-100602	61	111358-88-4	Lestaurtinib
25	1243583-88-1	CAY10669	62	778649-18-6	Butyrolactone 3
26	3690-10-6	Zebularine	63	1069-66-5	Valproic acid (sodium salt)
27	528-53-0	Delphinidin (chloride)	64	380315-80-0	Tenovin-1
28	732302-99-7	ITF 2357	65	1011557-82-6	Tenovin-6
29	1320288-19-4	UNC0631	66	156-54-7	Sodium butyrate
30	1320288-17-2	UNC0646	67	1808255-64-2	BIX01294 (hydrochloride hydrate)
31	1310877-95-2	Methylstat (hydrate)	68	16611-84-0	Anacardic acid
32	120964-45-6	3-Deazaneplanocin A (hydrochloride)	69	304896-28-4	AGK2
33	129-46-4	Suramin (sodium salt)	70	1045792-66-2	CAY10603
34	98-92-0	Nicotinamide	71	5690-03-9	Splitomicin
35	207671-42-9	2,4-Pyridinedicarboxylic Acid	72	174664-65-4	CBHA
36	1403764-72-6	PFI-1	73	251456-60-7	M 344
37	320-67-2	5-Azacytidine	74	151720-43-3	Oxamflatin

Table 1. Continue

Code	CAS number	Drug name	Code	CAS number	Drug name
75	1105698-15-4	Salermide	109	199596-05-9	JIB-04
76	299953-00-7	Mirin	110	1477949-42-0	CAY10683
77	937039-45-7	Pimelic diphenylamide 106	111	1346574-57-9	GSK126
78	940943-37-3	KD 5170	112	1446144-04-2	CPI-203
79	404950-80-7	Panobinostat	113	154-42-7	6-Thioguanine
80	209783-80-2	MS-275	114	1252003-15-8	Tubastatin A
81	926908-04-5	HNHA	115	1968-05-4	3,3'-Diindolylmethane
82	48208-26-0	RG-108	116	202590-98-5	OTX015
83	10302-78-0	2',3',5'-triacetyl-5-azacytidine	117	2140-61-6	5-Methylcytidine
84	979-92-0	S-adenosyl homocysteine	118	304896-21-7	AGK7
85	1197196-48-7	UNC0224	119	838-07-3	5-Methyl-2'-deoxycytidine
86	743420-02-2	Chidamide	120	1380288-87-8	EPZ5676
87	537049-40-4	Tubacin	121	852475-26-4	MC 1568
88	102052-95-9	3-Deazaneplanocin A (DZNep)	122	40951-21-1	α-Hydroxyglutaric acid (sodium salt)
89	58944-73-3	Sinefungin	123	52248-03-0	S-(5'-adenosyl)-L-methionine (tosylate)
90	382180-17-8	Pyroxamide	124	1044870-39-4	RVX-208
91	5262-39-5	N-oxalylglycine	125	1012054-59-9	CUDC-101
92	890190-22-4	WDR5-0103	126	404951-53-7	LAQ824
93	1396772-26-1	EPZ005687	127	300816-11-9	Nullscript
94	1561178-17-3	SGC0946	128	1431368-48-7	GSK-LSD1 (hydrochloride)
95	1415800-43-9	UNC1215	129	1357389-11-7	RGFP966
96	420831-40-9	AK-7	130	1440209-96-0	BRD73954
97	1346704-33-3	GSK343	131	501-36-0	Trans-resveratrol
98	1619994-69-2	Bromosporine	132	89464-63-1	DMOG
99	1619994-68-1	GSK2801	133	58880-19-6	Trichostatin A
100	14513-15-6	SIRT1/2 inhibitor IV	134	193551-00-7	CAY10398
101	2147701-33-3	I-CBP112 (hydrochloride)	135	1418131-46-0	RSC-133
102	1613695-14-9	SGC-CBP30	136	537034-17-6	BML-210
103	1481677-78-4	UNC0642	137	10083-24-6	Piceatannol
104	1431612-23-5	UNC1999	138	839699-72-8	CAY10591
105	1627607-87-7	(R)-PFI-2 (hydrochloride)	139	848193-68-0	EX-527
106	1429651-50-2	HPOB	140	149647-78-9	SAHA
107	96017-59-3	2-Hexyl-4-pentynoic acid	141	1986-47-6	2-PCPA (hydrochloride)
108	1819363-80-8	PFI-3			

2.2. Reagents

3-Deazaneplanocin A (DZNep) was purchased from Cayman Chemical (USA). Forskolin (Fsk) was purchased from were purchased from Sigma-Aldrich (USA).

2.3. Cell Culture

Cells were cultured at 37 ℃ under humidified air containing 5% CO_2 in a closed incubator. Murine melanoma B16/F10 cells (ATCC CRL-6475) were purchased from the American

Type Culture Collection (USA) and cultured in Dulbecco's modified Eagle's medium containing 10% fetal bovine serum (Gibco BRL, USA) and 1% antibiotics (100 U/mL penicillin, 0.1 mg/mL streptomycin, 0.25 ㎍/mL amphotericin B (Thermo Fisher, USA)).

2.4. Screening Assay for Melanin Synthesis

B16/F10 cells were seeded into 96 well culture plates (5×10^3 cells per well) and incubated for 24 h. The cells were then treated with 0.1 ㎛M of test drugs. Following drug treatment, overall melanin synthesis was estimated by measuring the optical density (OD) of each well (cells plus medium, without cell lysis) at 400 nm every 24 h up to 3 days using a Spectrostar Nano microplate reader (BMG LABTECH GmbH, Germany).

2.5. Cell Viability Assay

Cell viability was estimated using 3-(4,5-dimethylthiazol-2-yl)-2,5-diphenyltetrazolium bromide (MTT)[28,29]. The attached cells were washed with PBS and incubated in a 100 ㎕ growth medium containing 1 mg/mL MTT (Amresco, USA) for 2 h at 37 ℃. After removing the medium, cells were extracted with 100 ㎕ dimethyl sulfoxide and the OD was measured at 570 nm. Viable and dead cells were counted by the trypan blue exclusion assay[30]. Cells were harvested by trypsinization followed by centrifugation. The cells were suspended in a culture medium and mixed with 0.1% trypan blue solution (Sigma-Aldrich) at a one-to-one ratio. The numbers of stained dead cells and unstained viable cells were counted on a hemocytometer under a microscope.

2.6. Melanin and Protein Content Assays

The content of intracellular melanin was determined as previously described[28,29]. Cells were seeded into 6 well culture plates (1.0×10^5 cells per well) and incubated for 24 h. Then, the cells were treated with various concentrations of the test drugs for 72 h. The melanin was extracted from the cells with 1.0 N sodium hydroxide at 60 ℃ for 60 min. Melanin contents were determined by measuring the OD at 400 nm and normalized to the total protein content of the cells. The protein contents were determined using DC protein assay (Bio-Rad, USA).

2.7. Cellular TYR Activity Assay

After treatment of B16/F10 cells with drug, the TYR activity of cell lysates was determined by an indirect spectrophotometric method using L-tyrosine plus L-3,4-dihydroxyphenylalanine (L-DOPA) as the substrate[31,32]. Cells were extracted with an ice-cold lysis buffer containing 10 mM Tris-HCl (pH 7.4), 120 mM NaCl, 25 mM KCl, 2.0 mM EGTA, 1.0 mM EDTA, 0.5% Triton X-100, and a protease inhibitor cocktail (Roche, Germany), followed by centrifugation at 13,000 × g for 15 min at 4 ℃ to obtain a supernatant. The reaction mixture (200 ㎕) consisting of 100 mM sodium phosphate buffer (pH 6.8), 1.0 mM L-tyrosine, 42 ㎛M L-DOPA, and cell lysate (40 ㎍ protein) was incubated at 37 ℃. Changes in the OD at 475 nm were measured for the reaction mixture with cell lysates over time and corrected for the values obtained from the control reaction without cell lysates. The relative enzyme activity was calculated using the following formula: activity (percentage of the control) = (C-D)/(A-B) × 100, where A and B represent the OD changes of the control group over time, with and without cell lysates, respectively, while C and D represent the OD changes of the test group over time, with and without cell lysates, respectively.

2.8. Western Blot Analysis

Western blot analysis was performed as previously described[28, 33]. The primary antibody for TYR (#127217) was purchased from MyBioSource (USA), the primary antibodies for TYRP1 (#10443) and β-actin (#47778) were purchased from Santa Cruz Biotechnology (USA), and the primary antibody for DCT (#74073) was purchased from Abcam (UK). Anti-rabbit IgG (#2357) and anti-goat IgG (#2020) secondary antibodies were purchased from Santa Cruz Biotechnology, and anti-mouse IgG (#7076) secondary antibody was purchased from Cell Signaling Technology (USA). Antibodies were diluted in TBST (137 mM Sodium Chloride, 20 mM Tris, 0.1% Tween 20, pH 7.6.) containing 5% bovine serum albumin (BSA).

After B16/F10 cells were incubated with drugs, cell lysates were prepared using a lysis buffer consisting of 10 mM Tris-Cl (pH 7.4), 120 mM NaCl, 25 mM KCl, 2 mM EGTA, 1 mM EDTA, 0.5% Triton X-100, and a protease inhibitor cocktail. These cell lysates were used for the measurement of

TYR, TYRP1, and DCT expression. To determine MITF expression, cell lysates were prepared using RIPA buffer consisting of 25 mM Tris-HCl (pH 7.6), 150 mM NaCl, 1% NP-40, 1% sodium deoxycholate, 0.1% sodium dodecyl sulfate (SDS), and protease inhibitor cocktail. Each cell lysate (30 ㎍ protein) was mixed with 5 × SDS-PAGE loading buffer and heated at 95 ℃ for 5 min to denature the protein. Proteins were separated by SDS-polyacrylamide gel electrophoresis at 100 V on a gel containing 10% polyacrylamide and the proteins were transferred overnight at 4 ℃ to a polyvinylidene difluoride membrane (Amersham Pharmacia, UK). After blocking the membranes with TBST (137 mM Sodium chloride, 20 mM Tris, 0.1% Tween 20, pH 7.6.) containing 5% skim milk at room temperature for 1 h, the membrane was incubated with 1:1000 dilution of the primary antibody overnight at 4 ℃ followed by incubation with 1:2000 dilution of the secondary antibody conjugated with horseradish peroxidase for 1 h at 25 ℃. Antibody dilution buffer was TBST containing 5% bovine serum albumin (BSA). The target protein bands were detected by chemiluminescence using a picoEPD Western Reagent Kit (ELPIS-Biotech, Korea) and the blots were densitometrically analyzed using the NIH Image J program (USA).

2.9. Quantitative Reverse Transcription-Polymerase Chain Reaction (qRT-PCR) Analysis

After treatment of B16/F10 cells with drugs, cellular mRNA was extracted using the RNeasy kit (Qiagen, USA), and complementary DNA (cDNA) was synthesized from 1 ㎍ of RNA by reverse transcription using the cDNA kit (High-Capacity cDNA Archive Kit, Applied Biosystems, USA). The qRT-PCR analysis was performed with the StepOnePlus™ Real-time PCR System (Applied Biosystems). The reaction mixture (20 ㎕) consisted of SYBR Green PCR Master Mix (Applied Biosystems), cDNA (60 ng), and gene-specific primer sets (2 pmol) (Macrogen, Korea). The primer sequences are shown in Table 2.

Thermal cycling parameters for PCR were set as follows: initial incubation at 50 ℃ for 2 min, DNA polymerase activation at 95 ℃ for 10 min, 40 amplification cycles (annealing and extension at 60 ℃ for 1 min and melting at 95 ℃ for 15 s), and a dissociation step. Melting curves were generated to confirm the homogeneity of the amplified product. The mRNA level of each gene was normalized to the mRNA level of an internal standard, glyceraldehyde 3-phosphate dehydrogenase (GAPDH) using the relative Ct method[37]. Ct is defined as the number of PCR cycles required for the fluorescence signal to exceed the preset threshold level. Fold changes in the test group compared to the control group were calculated as 2^{-DDCt}, where $DDCt = DCt_{(test)} - DCt_{(control)} = [Ct_{(gene, test)} - Ct_{(reference, test)}] - [Ct_{(gene, control)} - Ct_{(reference, control)}]$.

2.10. Enzyme-linked Immunosorbent Assay (ELISA) for S-adenosylhomocysteine

After B16/F10 cells were treated with drugs, cells were extracted with an ice-cold lysis buffer consisting of 25 mM Tris-HCl (pH 7.6), 150 mM NaCl, 1% NP-40, 1% sodium deoxycholate, 0.1% SDS, and a protease inhibitor cocktail.

Table 2. Sequences of primers used for quantitative reverse transcriptase-polymerase chain reaction

Gene name	GenBank accession number	Primer sequences	References
TYR	NM_011661.5	Forward: 5'-CTTCTTCTCCTCCTGGCAGATC-3' Reverse: 5'-TGGGGGTTTTGGCTTTGTC-3'	[34]
TYRP1	NM_001282015.1	Forward: 5'-CAGTGCAGCGTCTTCCTGAG-3' Reverse: 5'-TTCCCGTGGGAGCACTGTAA-3'	[35]
DCT	NM_010024.3	Forward: 5'-GATGGCGTGCTGAACAAGGA-3' Reverse: 5'-ATAAGGGCCACTCCAGGGTC-3'	[35]
MITF	NM_008601.3	Forward: 5'-GCTGGAAATGCTAGAATACAG-3' Reverse: 5'-TTCCAGGCTGATGATGTCATC-3'	[34]
GAPDH	NM_001289726.1	Forward: 5'-GCATCTCCCTCACAATTTCCA-3' Reverse: 5'-GTGCAGCGAACTTTATTGATGG-3'	[36]

Levels of S-adenosylhomocysteine in the cell lysates were determined using an ELISA Kit (#STA-671-C) from Cell Biolabs, Inc. (USA). A standard curve was constructed using S-adenosylhomocysteine-BSA. Contents of S-adenosylhomocysteine were normalized to the total protein content of the cells.

2.11. Statistical Analysis

The experimental results of this study are expressed as the mean ± standard deviation (SD) of three or more independent experiments. All data were statistically analyzed by one-way analysis of variance (ANOVA) using SigmaStat v.3.11 Statistical Analysis Software (Systat Software Inc, USA). All experimental groups were compared with a single control group through Dunnett's test. p <0.05 was considered statistically significant.

3. Results

3.1. Screening Assays

An epigenetic screening library consisting of 141 cell-permeable small molecule drugs was used in the preliminary screening assay. B16/F10 murine melanoma cells were treated with each drug at 0.1 μM to monitor its effects on cellular melanin synthesis and cell viability. As shown in Figure 1, of the 141 different drugs tested, (−)-neplanocin A (#15), 3-deazaneplanocin A (DZNep) hydrochloride (#32), DZNep (#88) effectively increased cellular melanin synthesis without decreasing cell viability.

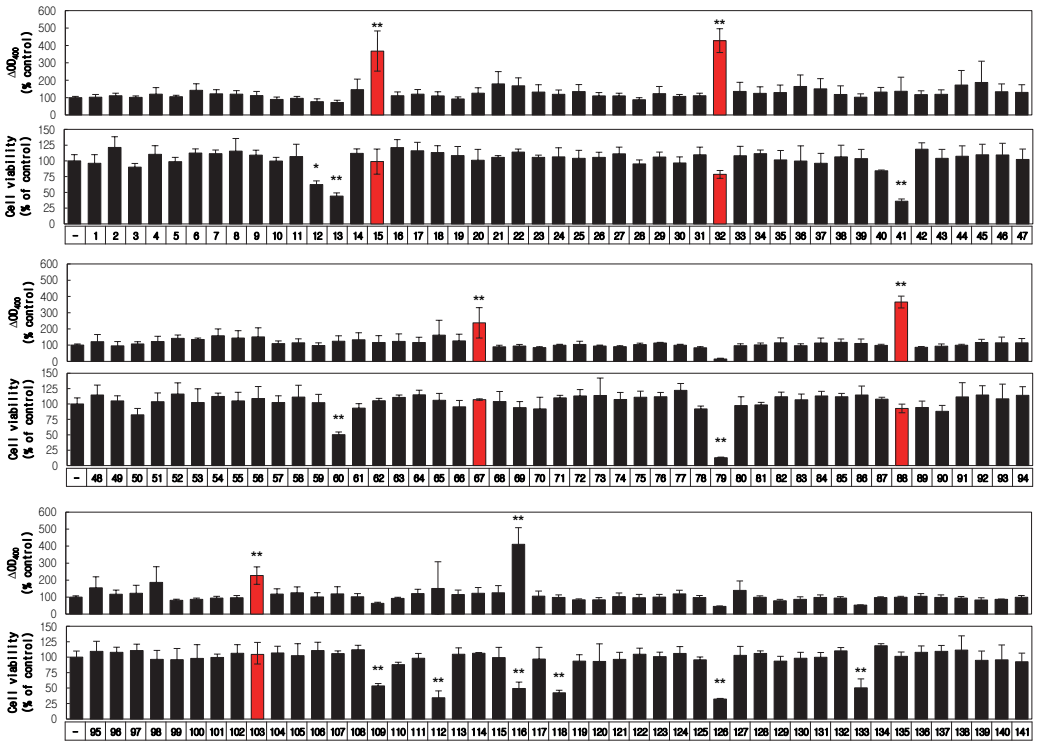

Figure 1. Effects of epigenetic drugs on cellular melanin synthesis and cell viability in B16/F10 cells. Cells were treated with each drug at 0.1 μM for 48 h for the cell viability assay using MTT and for 72 h for the melanin synthesis assay. Data are presented as percentages of the control values (mean ± SD, N = 3). All treatments (141 drugs) were compared to the vehicle (dimethyl sulfoxide) control using Dunnett's test with one-way ANOVA. $^{*}p < 0.05$, $^{**}p < 0.01$ versus control. Drugs that promoted melanin synthesis without causing cytotoxicity are marked with red color; (−)-neplanocin A (#15), DZNep hydrochloride (#32), and 3-deazaneplanocin A (DZNep, #88) are inhibitors of S-adenosylhomocysteine hydrolase; BIX01294 (hydrochloride hydrate) (#67) and UNC0642 (#103) are inhibitors of histone methyltransferase EHMT2.

3.2. Comparison of Three Selected Drugs

(−)-Neplanocin A (#15), 3-deazaneplanocin A (DZNep) hydrochloride (#32), and DZNep (#88) are structurally related drugs. These three drugs were compared by treating B16/F10 cells with each over a range of concentrations. The chemical structures and their dose-dependent effects on cellular melanin synthesis and cell viability are shown in Figure 2. Overall, they showed similar effects on cellular melanin synthesis and cell viability. DZNep (#88) was selected as a representative drug for subsequent experiments.

3.3. Effects of DZNep on Cell Viability and Intracellular Melanin Content

Time-dependent effects of DZNep on cell viability and intracellular melanin content were examined. B16/F10 cells were treated with DZNep or Fsk at the indicated concentrations for 24 h, 48 h, and 72 h. Viable cells and dead cells within the grids on a hemocytometer were counted. Cell viability is calculated as the number of viable cells divided by the total number of cells, and the data are shown in Figure 3A. As shown in Figure 3B, Fsk treatment at 1.0 μM increased the

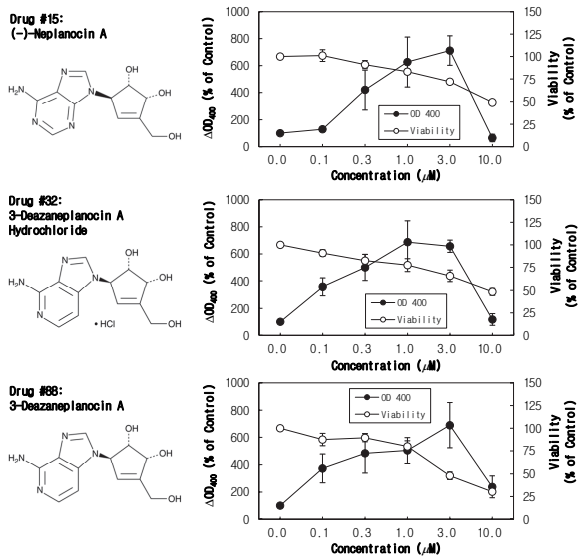

Figure 2. Dose-dependent effects of three drugs on the cellular melanin synthesis and cell viability of B16/F10 cells. Cells were treated with each drug at the indicated concentrations for 48 h in the cell viability assay using MTT and for 72 h in the melanin synthesis assay. Data are presented as percentages of the control values (mean ± SD, N = 3).

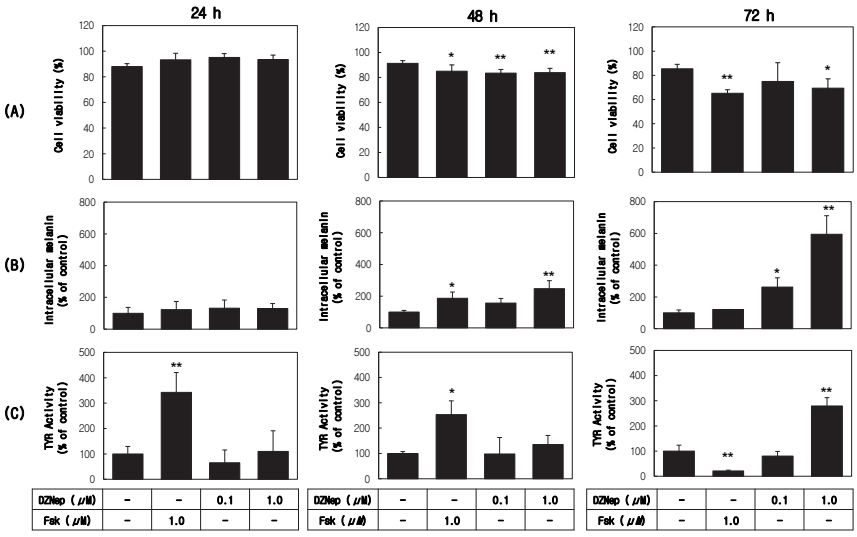

Figure 3. Effects of DZNep and Fsk on viability, intracellular melanin content, and cellular TYR activity of B16/F10 cells. Cells were treated with DZNep or Fsk at the indicated concentrations for 24 h, 48 h, and 72 h. (A) Viable and dead cells were counted by trypan blue exclusion assay. Cell viability was represented as the number of viable cells divided by the total number of cells (N = 3). (B) Intracellular melanin content was normalized to total protein contents (N = 6). (C) Cell lysates were used to measure TYR activity which was normalized to total protein content. Data are presented as mean ± SD. $^{*}p < 0.05$, $^{**}p < 0.01$ versus control.

melanin content of the cells compared with the controls at 48 h and then returned to the control level at 72 h, indicating that the effect is transient. In contrast, 1.0 μM of DZNep increased the melanin content of the cells at 48 h, to a level similar to 1.0 μM Fsk. DZNep at 1.0 μM increased the melanin content to a much higher level at 72 h. DZNep at 0.1 μM also increased the intracellular melanin content of the cells at 72 h. Overall, these results indicated that the promelanogenic effects of DZNep were slower, but more prolonged compared with those of Fsk.

3.4. Effects of DZNep on Cellular TYR Activity

The increase of melanin content in cells treated with DZNep or Fsk may be associated with the enhancement of melanin synthetic activity of the cells. To address this issue, the activity of TYR, a rate-limiting enzyme in the melanin synthetic pathway, was assessed using cell lysates from B16/F10 cells treated with DZNep or Fsk at the indicated concentrations for 24 h, 48 h, and 72 h. As shown in Figure 3C, Fsk increased cellular TYR activity 24 to 48 h after drug treatment, and then decreased it to a very low level at 72 h. In contrast, DZNep increased cellular TYR activity gradually and the increase was statistically significant at 72 h after treatment with 1.0 μM DZNep.

3.5. Effects of DZNep on the Protein Levels of Melanogenic Enzymes

To examine whether DZNep or Fsk increases protein expression of TYR and other melanogenic enzymes, such as TYRP1 and DCT, western blot analysis was performed using cell lysates from the B16/F10 cells treated with DZNep or Fsk at the indicated concentrations for 48 h and 72 h. As shown in Figure 4, treatment with 1.0 μM Fsk or 1.0 μM DZNep for

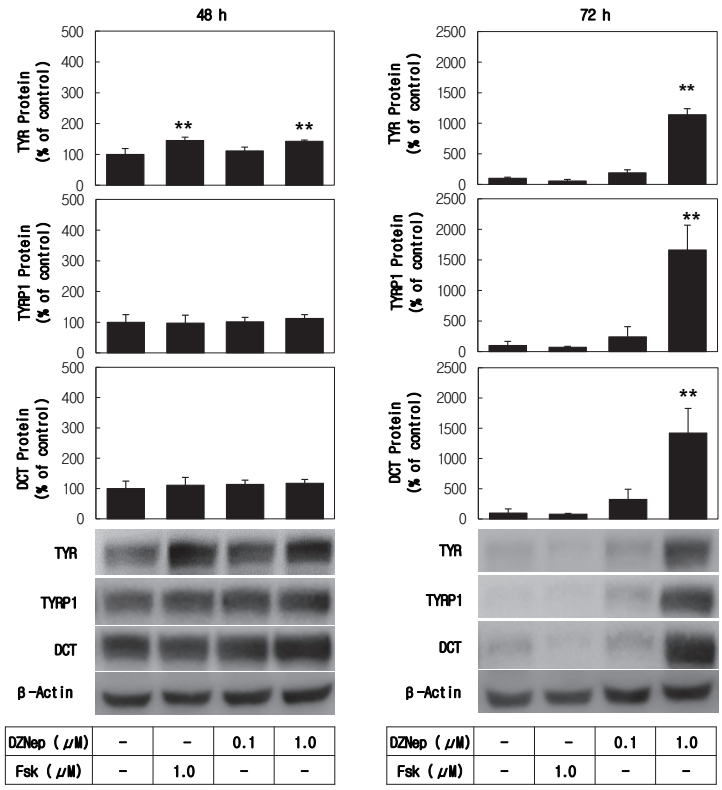

Figure 4. Effects of DZNep and Fsk on the protein levels of TYR, TYRP1, and DCT in B16/F10 cells. Cells were treated with DZNep or Fsk at the indicated concentrations for 48 h and 72 h. Cell lysates were used for western blot analysis with β-actin as a loading control. Typical blot images are shown. Data are presented as percentages of the control values (mean ± SD, N = 3). $^{*}p < 0.05$, $^{**}p < 0.01$ versus control.

48 h increased TYR protein levels slightly, but they had no significant effects on TYRP1 and DCT protein levels. At 72 h, 1.0 μM DZNep significantly increased the levels of TYR, TYRP1, and DCT proteins markedly.

3.6. Effects of DZNep on the mRNA Levels of Melanogenic Enzymes

To examine whether DZNep or Fsk affects mRNA levels of melanogenic enzymes such as TYR, TYRP1, and DCT, qRT-PCR was performed using total RNA extracted from B16/F10 cells treated with DZNep or Fsk at the indicated concentrations for 6, 12, 24, and 48 h. As shown in Figure 5, treatment with 1.0 μM Fsk increased TYR and TYRP1 mRNA at 12 h and 24 h. DCT was unaffected by Fsk. DZNep at 1.0 μM increased the mRNA levels of TYR, TYRP1, and DCT at 24 and 48 h. DZNep at 0.1 μM increased the mRNA level of TYRP1 at 24 h, and that of TYR and TYRP1 at 48 h. These results indicate that DZNep and Fsk can induce the expression of TYR and TYRP1 in different time courses.

3.7. Effects of DZNep on MITF Protein and mRNA Levels

To examine a potential association of MITF in the promotion of melanogenesis by DZNep, B16/F10 cells were treated with DZNep or Fsk at the indicated concentrations for 24 or 48 h, and western blot analysis was performed to determine MITF protein levels. As shown in Figure 6A, treatment with DZNep at 0.1 to 1.0 μM increased MITF protein levels at 48 h.

Additionally, MITF mRNA levels were determined for B16/F10 cells treated with DZNep or Fsk at the indicated concentrations for 6, 12, 24, and 48 h. As shown in Figure 6B, treatment with 1.0 μM Fsk resulted in an increase of MITF mRNA at 6 and 12 h. DZNep at 1.0 μM increased the mRNA levels of MITF at 48 h. These results indicate that DZNep and Fsk can induce MITF expression in different time courses.

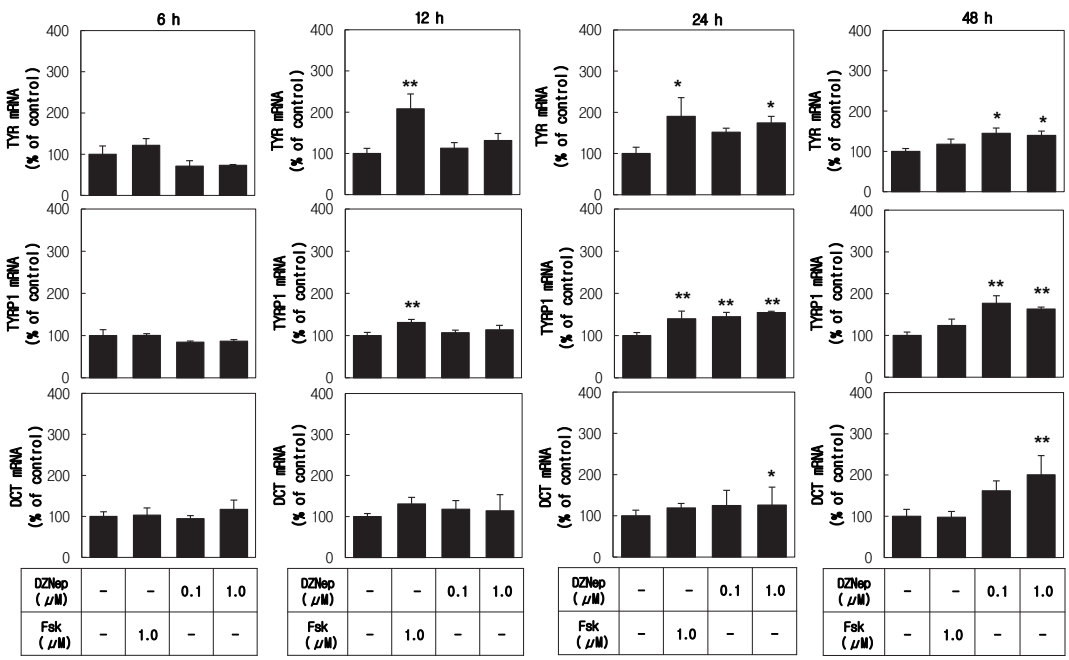

Figure 5. Effects of DZNep and Fsk on the mRNA levels of TYR, TYRP1, and DCT in B16/F10 cells. Cells were treated with DZNep or Fsk at the indicated concentrations for 6, 12, 24, and 48 h. The mRNA levels of TYR, TYRP1, and DCT were determined by qRT-PCR and normalized to GAPDH. Data are presented as the percentage of the control values (mean ± SD, N = 3). $^{*}p < 0.05$, $^{**}p < 0.01$ versus control.

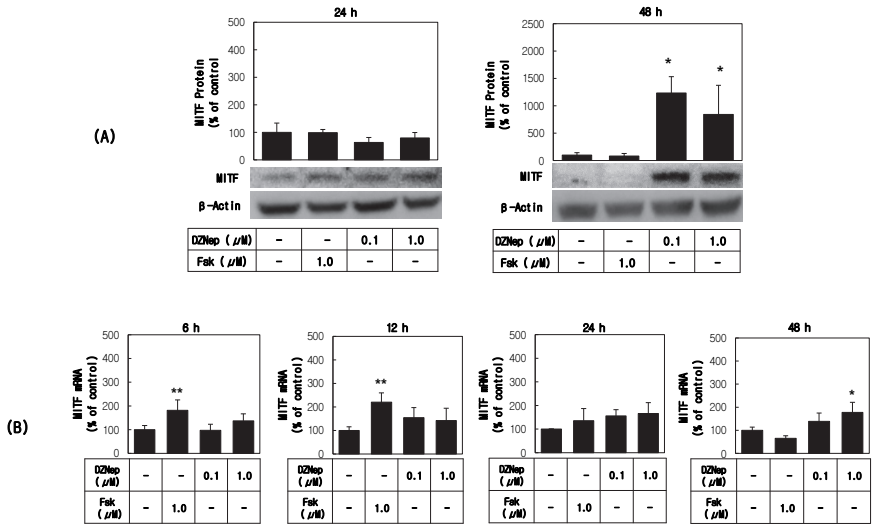

Figure 6. Effects of DZNep and Fsk on MITF protein and mRNA levels in B16/F10 cells. Cells were treated with DZNep or Fsk at the indicated concentrations for 48 h. (A) Cell lysates were used for western blot analysis with β-actin as a loading control. Typical blot images are shown. (B) MITF mRNA levels were measured by qRT-PCR and normalized to GAPDH. Data are presented as the percentage of the control values (mean ± SD, N = 3). $^{*}p < 0.05$ versus control.

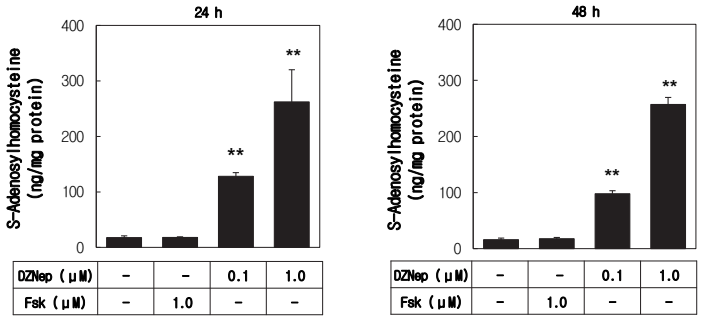

Figure 7. Effects of DZNep and Fsk on the contents of S-adenosylhomocysteine in B16/F10 cells. Cells were treated with DZNep or Fsk at the indicated concentrations for 24 h and 48 h. The contents of S-adenosylhomocysteine in cell lysates were determined by a competitive ELISA. Data are presented as means ± SD (N = 3). $^{**}p < 0.01$ versus control.

3.8. Effects of DZNep on the Content of S-Adenosylhomocysteine

In the next experiment, B16/F10 cells were treated with DZNep or Fsk at the indicated concentrations for 24 h or 48 h, and the contents of S-adenosylhomocysteine in cell lysates were measured. As shown in Figure 7, treatment with DZNep at 0.1 and 1.0 μM increased S-adenosylhomocysteine levels markedly, whereas treatment with Fsk at 1.0 μM did not display such effects.

4. Discussion

From a drug library screen consisting of 141 epigenetic modulators, 3-deazaneplanocin A (DZNep, #88) and its analogs, (−)-neplanocin A (#15) and DZNep hydrochloride (#32), were identified as promoting melanin synthesis in B16/F10 murine melanoma cells. Promelanogenic effects of these drugs were observed at a concentration range from 0.1 to 3 μM. These effects did not result from toxic effects although significant cytotoxicity was observed at

concentrations higher than 3 μM. DZNep was chosen as a structurally representative drug for additional experiments in the present study. DZNep hydrochloride is a salt form of DZNep, and (−)-Neplanocin A has an additional nitrogen atom compared with the others. There were minor differences among these drugs in terms of pro-melanogenic activity and cytotoxicity.

Experimental evidence suggests that the promelanogenic effect of DZNep is associated with increased activity of the TYR enzyme in cells. In support of this, protein levels of the representative melanogenic enzymes, such as TYR, TYRP1, and DCT, were higher compared with those in control cells. Increases in the protein levels of these melanogenic enzymes are believed to result from the induction of gene expression by the drug. Consistently, the mRNA levels of TYR, TYRP1, and DCT were upregulated by drug treatment in a dose- and time-dependent manner. In addition, MITF protein and mRNA levels increased with drug treatment, suggesting that this transcription factor mediates the expression of melanogenic enzymes induced by DZNep.

In the present study, Fsk, a diterpene activator of adenylate cyclase found in the roots of Coleus forskohlii, was used as a positive control[38]. Previously, this compound was shown to increase melanin levels and reduce the incidence of skin cancer in mice exposed to UV radiation[39]. As expected, Fsk stimulated the melanin synthesis and the expression of TYR, TYRP1, and DCT as well as MITF. Fsk and DZNep displayed different time courses during the stimulation of melanin synthesis, suggesting that the mechanism of action may be different despite both drugs enhancing the expression of melanogenic enzymes as well as MITF. DZNep exhibited prolonged effects compared with Fsk.

DZNep is known as an inhibitor of S-adenosylhomocysteine hydrolase[26]. In the homocysteine metabolic pathway, S-adenosylhomocysteine hydrolase catalyzes the reversible hydrolysis of S-adenosylhomocysteine to homocysteine and adenosine[27]. Homocysteine can be methylated to methionine by acquiring a methyl group from N-5-methylenetetrahydrofolate. Methionine is then activated to S-adenosylmethionine which serves as a universal methyl donor for a variety of methylation reactions. S-adenosylhomocysteine is regenerated from these reactions and becomes available for S-adenosylhomocysteine hydrolase. Inhibition of S-adenosylhomocysteine hydrolase by DZNep results in an elevation of S-adenosylhomocysteine in cells[26].

Treatment of B16/F10 cells with DZNep was confirmed to increase S-adenosylhomocysteine in this study. A high concentration of S-adenosylhomocysteine can inhibit histone methyltransferase EZH2 (enhancer of zeste homolog 2), which catalyzes mono-, di-, and tri-methylation of lysine^{27} on histone H3 (H3K27Me1, H3K27Me2, and H3K27Me3) by transferring a methyl group from the cofactor S-adenosylmethionine[40, 41]. Therefore, histone methyltransferase EZH2 is a possible mediator in the promotion of melanogenesis by DZNep.

In the present study, BIX01294 (hydrochloride hydrate) (#67) and UNC0642 (#103) also displayed significant pro- melanogenic activities without causing cytotoxic effects. These drugs are known as potent and selective inhibitors of histone methyltransferase EHMT2 (Euchromatic histone-lysine N-methyltransferase 2), also called G9a, which catalyzes the mono- and di-methylation of histone H3 at lysine^{9} (H3K9me1 and H3K9me2) and lysine^{27}(H3K27me1 and H3K27me2)[42, 43]. Therefore, histone methyltransferase EHMT2 has the potential to play a role in the epigenetic regulation of melanogenesis.

Interestingly, a previous study reported that S-adenosylhomocysteine hydrolase was upregulated in the vitiliginous skin[44]. Some reports suggested the association of increased homocysteine levels with hypopigmentation disorders[45,46]. Serum homocysteine levels were highly elevated in vitiligo patients[47]. The production of toxic reactive oxygen species by homocysteine oxidation was shown to induce apoptosis of melanocytes[48]. Homocysteine exerted an inhibitory effect on TYR enzyme activity, probably by chelating copper at the active site of the enzyme[49]. Thus, an increase in local homocysteine concentration can interfere with normal melanogenesis and the survival of melanocytes.

A hypothetical mechanism of action of DZNep in stimulating melanin synthesis is proposed in Figure 8. The inhibition of S-adenosylhomocysteine hydrolase by DZNep leads to the accumulation of S-adenosylhomocysteine and the subsequent inhibition of the activities of histone methyltransferases, such as EZH2 and EHMT2. The chromatin structure is then modified due to histone H3 demethylation and enhances the transcription of MITF or other target genes involved in melanogenesis.

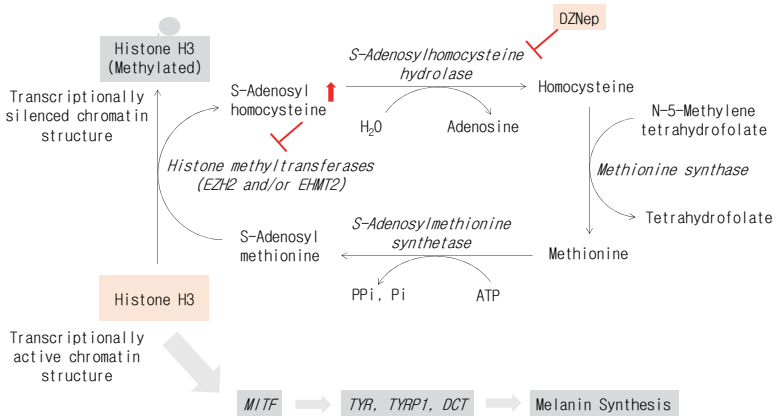

Figure 8. A hypothetical mechanism of action for promelanogenic effects of DZNep. DZNep inhibits S-adenosylhomocysteine hydrolase and causes the accumulation of S-adenosylhomocysteine. A high concentration of S-adenosylhomocysteine inhibits histone methyltransferases EZH2 and/or EHMT2, which catalyze methylation of lysine residues on histone H3. The resultant decrease in histone H3 methylation modifies the chromatin structure from a transcriptionally silenced form to an active form. Such change in chromatin structure enhances the expression of MITF, which in turn induces the expression of TYR, TYRP1, and DCT involved in melanin synthesis.

5. Conclusion

In conclusion, this study identified DZNep that promotes melanin synthesis in B16/F10 cells by inducing the expression of melanogenic enzymes, such as TYR, TYRP1, and DCT, through a MITF-mediated mechanism. This study also suggests that melanogenesis can be epigenetically modulated by targeting S-adenosylhomocysteine hydrolase in certain cellular contexts. Further studies are needed to examine whether histone methyltransferases EZH2 and/or EHMT2 are directly involved in the regulation of melanogenesis.

Acknowledgments

This work was supported by the National Research Foundation of Korea (NRF) grant funded by the Korea government (Ministry of Science and ICT) (No. 2019R1I1A2A01045132), Republic of Korea.

References

1. R. Ganceviciene, A. I. Liakou, A. Theodoridis, E. Makrantonaki, and C. C. Zouboulis, Skin anti-aging strategies, Dermatoendocrinol., 4(3), 308 (2012).
2. M. Ramos-e-Silva, L. R. Celem, S. Ramos-e-Silva, and A. P. Fucci-da-Costa, Anti-aging cosmetics: Facts and controversies, *Clin. Dermatol.,* **31**(6), 750 (2013).
3. P. T. Rose, Pigmentary disorders, *Med. Clin. North. Am.,* **93**(6), 1225 (2009).
4. V. D. Callender, S. St Surin-Lord, E. C. Davis, and M. Maclin, Postinflammatory hyperpigmentation: etiologic and therapeutic considerations, *Am. J. Clin. Dermatol.,* **12**(2), 87 (2011).
5. P. Ganju, S. Nagpal, M. H. Mohammed, P. Nishal Kumar, R. Pandey, V. T. Natarajan, S. S. Mande, and R. S. Gokhale, Microbial community profiling shows dysbiosis in the lesional skin of vitiligo subjects, *Sci. Rep.,* **6**, 18761 (2016).
6. R. A. Spritz and G. H. Andersen, Genetics of vitiligo, *Dermatol. Clin.,* **35**(2), 245 (2017).
7. M. B. C. Maymone, H. H. Neamah, E. A. Secemsky, and N. A. Vashi, Correlating the dermatology life quality index and skin discoloration impact evaluation questionnaire tools in disorders of hyperpigmentation, *J. Dermatol.,* **45**(3), 361 (2018).
8. J. D. Simon, D. Peles, K. Wakamatsu, and S. Ito, Current challenges in understanding melanogenesis: bridging chemistry, biological control, morphology, and function, *Pigment Cell Melanoma Res.,* **22**(5), 563 (2009).

9. C. Olivares and F. Solano, New insights into the active site structure and catalytic mechanism of tyrosinase and its related proteins, *Pigment Cell Melanoma Res.,* **22**(6), 750 (2009).
10. M. V. Schiaffino, Signaling pathways in melanosome biogenesis and pathology, *Int. J. Biochem. Cell Biol.,* **42**(7), 1094 (2010).
11. A. Slominski, D. J. Tobin, S. Shibahara, and J. Wortsman, Melanin pigmentation in mammalian skin and its hormonal regulation, *Physiol. Rev.,* **84**(4), 1155 (2004).
12. Y. C. Boo, Up- or downregulation of melanin synthesis using amino acids, peptides, and their analogs, *Biomedicines,* **8**(9), 322 (2020).
13. Y. C. Boo, Human skin lightening efficacy of resveratrol and its analogs: from *in vitro* studies to cosmetic applications, *Antioxidants,* **8**(9), 332 (2019).
14. Y. C. Boo, p-coumaric acid as an active ingredient in cosmetics: a review focusing on its antimelanogenic effects, *Antioxidants,* **8**(8), 275 (2019).
15. C. Niu and H. A. Aisa, Upregulation of melanogenesis and tyrosinase activity: potential agents for vitiligo, *Molecules,* **22**(8), 1303 (2017).
16. T. Pillaiyar, V. Namasivayam, M. Manickam, and S. H. Jung, Inhibitors of melanogenesis: an updated review, *J. Med. Chem.,* **61**(17), 7395 (2018).
17. Y. C. Boo, Emerging strategies to protect the skin from ultraviolet rays using plant-derived materials, *Antioxidants,* **9**(7), 637 (2020).
18. K. D. Haltaufderhyde and E. Oancea, Genome-wide transcriptome analysis of human epidermal melanocytes, *Genomics,* **104**(6 Pt B), 482 (2014).
19. M. Soejima and Y. Koda, Population differences of two coding SNPs in pigmentation-related genes SLC24A5 and SLC45A2, *Int. J. Legal Med.,* **121**(1), 36 (2007).
20. J. B. Cheng and R. J. Cho, Genetics and epigenetics of the skin meet deep sequence, *J. Invest. Dermatol.,* **132**(3 Pt 2), 923 (2012).
21. J. S. Shin, H. S. Jeong, M. K. Kim, H. Y. Yun, K. J. Baek, N. S. Kwon, and D. S. Kim, The DNA methylation inhibitor 5-azacytidine decreases melanin synthesis by inhibiting CREB phosphorylation, *Pharmazie,* **70**(10), 646 (2015).
22. S. Yokoyama, E. Feige, L. L. Poling, C. Levy, H. R. Widlund, M. Khaled, A. L. Kung, and D. E. Fisher, Pharmacologic suppression of MITF expression via HDAC inhibitors in the melanocyte lineage, *Pigment Cell Melanoma Res.,* **21**(4), 457 (2008).
23. K. H. Kim, B. H. Bin, J. Kim, S. E. Dong, P. J. Park, H. Choi, B. J. Kim, S. J. Yu, H. Kang, H. H. Kang, E. G. Cho, and T. R. Lee, Novel inhibitory function of miR-125b in melanogenesis, *Pigment Cell Melanoma Res.,* **27**(1), 140 (2014).
24. K. H. Kim, T. R. Lee, and E. G. Cho, SH3BP4, a novel pigmentation gene, is inversely regulated by miR-125b and MITF, *Exp. Mol. Med.,* **49**(8), e367 (2017).
25. H. Song, Y. J. Hwang, J. W. Ha, and Y. C. Boo, Screening of an epigenetic drug library identifies 4-((hydroxyamino) carbonyl)-N-(2-hydroxyethyl)-N-phenyl -benzeneacetamide that reduces melanin synthesis by inhibiting tyrosinase activity independently of epigenetic mechanisms, *Int. J. Mol. Sci.,* **21**(13), 4589 (2020).
26. R. I. Glazer, K. D. Hartman, M. C. Knode, M. M. Richard, P. K. Chiang, C. K. Tseng, and V. E. Marquez, 3-Deazaneplanocin: a new and potent inhibitor of S-adenosylhomocysteine hydrolase and its effects on human promyelocytic leukemia cell line HL-60, Biochem. Biophys. Res. Commun., 135(2), 688 (1986).
27. J. Selhub, Homocysteine metabolism, *Annu. Rev. Nutr.,* **19**, 217 (1999).
28. J. K. Seok, S. W. Lee, J. Choi, Y. M. Kim, and Y. C. Boo, Identification of novel antimelanogenic hexapeptides via positional scanning of a synthetic peptide combinatorial library, *Exp. Dermatol.,* **26**(8), 742 (2017).
29. J. H. Kim, J. K. Seok, Y. M. Kim, and Y. C. Boo, Identification of small peptides and glycinamide that inhibit melanin synthesis using a positional scanning synthetic peptide combinatorial library, *Br. J. Dermatol.,* **181**(1), 128 (2019).
30. S. A. Altman, L. Randers, and G. Rao, Comparison of trypan blue-dye exclusion and fluorometric assays for mammalian-cell viability determinations, *Biotechnol. Prog.,* **9**(6), 671 (1993).
31. A. Garcia-Jimenez, J. A. Teruel-Puche, J. Berna, J. N. Rodriguez-Lopez, J. Tudela, and F. Garcia-Canovas,

Action of tyrosinase on alpha and beta-arbutin: A kinetic study, *PLoS One,* **12**(5), e0177330 (2017).

32. S. W. Lee, J. H. Kim, H. Song, J. K. Seok, S. S. Hong, and Y. C. Boo, Luteolin 7-sulfate attenuates melanin synthesis through inhibition of CREB- and MITF-mediated tyrosinase expression, *Antioxidants,* **8**(4), 87 (2019).
33. S. M. An, J. S. Koh, and Y. C. Boo, Inhibition of melanogenesis by tyrosinase siRNA in human melanocytes, *BMB Rep.,* **42**(3), 178 (2009).
34. R. Yang, Y. Zheng, L. Li, S. Liu, M. Burrows, Z. Wei, A. Nace, M. Herlyn, R. Cui, W. Guo, G. Cotsarelis, and X. Xu, Direct conversion of mouse and human fibroblasts to functional melanocytes by defined factors, *Nat. Commun.,* **5**, 5807 (2014).
35. G. Y. Seo, Y. Ha, A. H. Park, O. W. Kwon, and Y. J. Kim, *Leathesia difformis* extract inhibits alpha-MSH-induced melanogenesis in B16F10 cells via down-regulation of CREB signaling pathway, *Int. J. Mol. Sci.,* **20**(3), 536 (2019).
36. M. S. Han, X. Che, G. H. Cho, H. R. Park, K. E. Lim, N. R. Park, J. S. Jin, Y. K. Jung, J. H. Jeong, I. K. Lee, S. Kato, and J. Y. Choi, Functional cooperation between vitamin D receptor and Runx2 in vitamin D-induced vascular calcification, *Plos One,* **8**(12), e83584 (2013).
37. K. J. Livak and T. D. Schmittgen, Analysis of relative gene expression data using real-time quantitative PCR and the $2^{-\Delta\Delta Ct}$ method, *Methods,* **25**(4), 402 (2001).
38. K. B. Seamon, W. Padgett, and J. W. Daly, Forskolin: unique diterpene activator of adenylate cyclase in membranes and in intact cells, *Proc. Natl. Acad. Sci. U S A,* **78**(6), 3363 (1981).
39. J. A. D'Orazio, T. Nobuhisa, R. Cui, M. Arya, M. Spry, K. Wakamatsu, V. Igras, T. Kunisada, S. R. Granter, E. K. Nishimura, S. Ito, and D. E. Fisher, Topical drug rescue strategy and skin protection based on the role of Mc1r in UV-induced tanning, *Nature,* **443**(7109), 340 (2006).
40. T. B. Miranda, C. C. Cortez, C. B. Yoo, G. N. Liang, M. Abe, T. K. Kelly, V. E. Marquez, and P. A. Jones, DZNep is a global histone methylation inhibitor that reactivates developmental genes not silenced by DNA methylation, *Mol. Cancer Ther.,* **8**(6), 1579 (2009).
41. A. Hayden, P. W. M. Johnson, G. Packham, and S. J. Crabb, S-adenosylhomocysteine hydrolase inhibition by 3-deazaneplanocin A analogues induces anti-cancer effects in breast cancer cell lines and synergy with both histone deacetylase and HER2 inhibition, *Breast Cancer Res. Treat.,* **127**(1), 109 (2011).
42. F. Liu, D. Barsyte-Lovejoy, F. L. Li, Y. Xiong, V. Korboukh, X. P. Huang, A. Allali-Hassani, W. P. Janzen, B. L. Roth, S. V. Frye, C. H. Arrowsmith, P. J. Brown, M. Vedadi, and J. Jin, Discovery of an in vivo chemical probe of the lysine methyltransferases G9a and GLP, *J. Med. Chem.,* **56**(21), 8931 (2013).
43. Z. Y. Lu, H. R. Salwen, J. U. Raj, and Q. W. Yang, Histone lysine methyltransferase EHMT2 is involved in proliferation, apoptosis, and DNA methylation of human neuroblastoma cells, *Cancer Res.,* **72**((2012).
44. R. Dey-Rao and A. A. Sinha, Interactome analysis of gene expression profile reveals potential novel key transcriptional regulators of skin pathology in vitiligo, *Genes Immun.,* **17**(1), 30 (2016).
45. S. Singh, U. Singh, and S. S. Pandey, Increased level of serum homocysteine in vitiligo, *J. Clin. Lab. Anal.,* **25**(2), 110 (2011).
46. J. Silverberg, and N. Silverberg, Serum homocysteine is associated with extent of vitiligo vulgaris, *J. Am. Acad. Dermatol.,* **64**(2), Ab142 (2011).
47. T. Y. Tsai, C. Y. Kuo, and Y. C. Huang, Serum homocysteine, folate, and vitamin B-12 levels in patients with vitiligo and their potential roles as disease activity biomarkers: A systematic review and meta-analysis, *J. Am. Acad. Dermatol.,* **80**(3), 646 (2019).
48. J. Chen, T. Zhuang, J. Chen, Y. Tian, X. Yi, Q. Ni, W. Zhang, P. Song, Z. Jian, L. Liu, T. Cui, K. Li, T. Gao, C. Li, and S. Li, Homocysteine induces melanocytes apoptosis via PERK-eIF2alpha-CHOP pathway in vitiligo, *Clin. Sci. (Lond),* **134**(10), 1127 (2020).
49. O. Reish, D. Townsend, S. A. Berry, M. Y. Tsai, and R. A. King, Tyrosinase inhibition due to interaction of homocysteine with copper - the mechanism for reversible hypopigmentation in homocystinuria due to cystathionine beta-synthase deficiency, *Am. J. Hum. Genet.,* **57**(1), 127 (1995).